

AUTOMATED SEGMENTATION OF THORACIC AORTA IN NON-CONTRAST CT IMAGES

Uday Kurkure, Olga C. Avila-Montes, Ioannis A. Kakadiaris

Computational Biomedicine Lab, University of Houston, Houston, TX

ABSTRACT

Aortic calcification has been shown to be related to cardiovascular disease. In this paper, we present a novel method for localization and segmentation of thoracic aorta in non-contrast CT images using dynamic programming concepts to detect and quantify aortic calcium. The localization and segmentation of the aorta are formulated as optimal path detection problems, which are solved using dynamic programming principles. We apply these methods on Hough space for aorta localization and a transformed polar coordinate space for aorta segmentation. We evaluate the proposed approach by comparing it with the manual annotations in terms of aorta location, boundary distance, and volume overlap.

Index Terms— Aorta, segmentation, CT

1. INTRODUCTION

Coronary heart disease (CHD) is the primary cause of morbidity and mortality in western societies. Studies have shown that calcification of the thoracic aorta, aortic arch, and aortic valve are associated with increased risk of cardiovascular disease [1, 2]. Prior to including aortic calcium measurements in cardiovascular risk assessment, longitudinal studies need to be conducted to assess the incremental value of thoracic aorta calcium in addition to coronary artery calcium (CAC). Aortic and coronary artery calcification can be quantified by non-contrast cardiac computed tomography (CT) [3]. Thoracic aorta calcification can be measured from standard cardiac CAC scans, without requiring any additional scanning, which is especially advantageous for retrospective studies. Currently, manual annotation of calcified plaques is the primary means of extracting quantitative information from non-contrast cardiac CT images. However, manual tracing is labor intensive and time consuming. Automated aortic¹ calcium detection and quantification requires automated methods for localization and segmentation of the ascending and descending aorta. Considerable research has been conducted towards aorta segmentation in Magnetic Resonance (MR) images [4, 5] but to the best of our knowledge there is no automated method that addresses aorta segmentation in cardiac CT scans. This might be attributed to the nature of the non-

contrast CT imaging, which suffers from lack of contrast between blood pool regions, muscle walls and pericardial fat, rendering the aorta segmentation quite a challenging task.

In this paper we describe a novel automated method for segmentation of the thoracic aorta in non-contrast cardiac CT images and posterior quantification of aortic calcified plaque. We use dynamic programming concepts to reformulate the problems of localizing and segmenting the thoracic aorta as optimal path detection problems constrained by certain cost functions. The proposed method has two main steps: First, the approximate position and size of the aorta are estimated by exploiting the circular shape of the aorta in axial images. We propose a novel method for aorta localization using Hough space as a medialness feature space and applying dynamic programming on that space to find the points corresponding to the center of the aorta in subsequent axial slices. In the second step, we use the estimated position and size of the aorta to detect refined aortic boundary contours using dynamic programming methods. We compare the results of our proposed method with manual annotations performed by an expert for geometric (aorta location and boundary) validations.

This rest of the paper is organized as follows: Section 2 provides a detailed description of the proposed algorithms for automated localization and segmentation of aorta. In Section 3, we present validation results on clinical data, and finally we conclude in Section 4.

2. METHODS

The input data are 3D non-contrast cardiac CT volumes organized as a stack of 2D axial slices. The vertical range of the CT volume is assumed to span from the level of pulmonary artery split at the base of the heart to the appearance of the diaphragm at the apex of the heart.

2.1. Localization of Thoracic Aorta

The first step towards automated segmentation of the thoracic aorta is to locate the position and estimate the size of the aorta in the thoracic CT scans. In spite of heart dynamics, the aorta maintains its global tubular shape with minor local deformations. Since the thoracic aorta runs vertically, its appearance in axial slices approximates a circular shape which is extracted using Hough transform. A dynamic programming

¹Following references to 'aorta' imply both ascending and descending aorta.

method is applied on the Hough spaces of subsequent axial slices to obtain a series of optimal best-fit circles for the aorta.

2.1.1. Computation of Hough Space

The Hough space is computed by performing a convolution operation using a circular kernel of radius r , $H = E \otimes K$, where H is the Hough space, E is the edge response, and K is the circular kernel. The edge response is computed using the canny edge detector. However, to emphasize image features and reduce the effect of spurious small edges, a non-linear gray-scale modification is performed by piecewise linear mapping models. To further smooth the regions of interest and preserve the edge information, anisotropic diffusion [6] is performed. Figures 1(a,b) depict the original and enhanced images, respectively. Since the size of the aorta varies for different individuals, multiple convolution operations are performed with different kernel radii. Also, instead of applying the Hough transform on the whole image and selecting two circles corresponding to the ascending and descending aortas, we apply Hough transform on two different regions of interest computed from the anatomical knowledge of relative location of the ascending and the descending aortas w.r.t. the lungs. The most probable circles appear as maxima in the Hough space. However, the global maximum point does not always correspond to the circle of interest (COI) (Fig. 1(c)). To overcome this issue, we use a dynamic programming-based approach to estimate position and size of the aorta in a series of 2D images.

2.1.2. Aorta Location Estimation using Dynamic Programming

To estimate the aortic COIs, we exploit the anatomical property that the thoracic aorta runs vertically and assume that there is little deviation in cross-sectional size and horizontal positioning of the aorta in subsequent axial slices. The goal is to select a single point, from the Hough space of each axial image, that corresponds to the aorta. In terms of dynamic programming, the problem is reformulated to find an optimal combination of points from the Hough spaces by minimizing a cost function. If there are N axial images in consideration, the solution of dynamic programming is a set \mathbf{P} of N points $(P_1, P_2, P_3, \dots, P_N) \in \mathbf{P}$, where each point P_i is represented by x-coordinate, y-coordinate, radius, and z-coordinate (x, y, r, z) . To obtain an optimal combination of points, the set \mathbf{P} should have minimum cost for the cost function, $C_s = \sum_{i=1}^N C(P_i)$. The cost associated with each point is given by,

$$C(P_i) = \omega_c C_c(P_{i-1}, P_i) + \omega_r C_r(P_{i-1}, P_i) + \omega_v C_v(P_i),$$

where C_c , C_r , and C_v are the cost component terms associated with the change in horizontal position of circles in adjacent axial slices, the change in radius of circles in adjacent axial slices, and the Hough value of points in Hough space respectively. The weights for the respective cost components

are ω_c , ω_r , and ω_v . The term C_c imposes 3D continuity of medial axis of aorta by constraining the amount of horizontal shift allowed for aortic circles in adjacent axial slices. The term C_r imposes a smooth tubular shape by restricting the amount of change in size of aortic circles allowed in adjacent axial slices. The term C_v forces selection of circle points with maximum edge points. Such a dynamic programming scheme allows us to avoid an exhaustive search for the optimal combination of circle points. To further reduce the computational cost, we limit our search to M points in each Hough space with maximum Hough value. This reduces our search space from $U \times V \times W \times N$ points (U and V are the x and y dimensions axial image and W is the number of different radii considered) to $M \times N$ points. The weights of different cost component terms in the cost function are obtained experimentally. Figure 1(d) depicts an accurately detected circle from the Hough space using the dynamic programming method.

2.2. Aortic Boundary Contour Detection using Dynamic Programming

The goal of this step is to compute refined aortic boundary contours using the position and size estimates from the previous step. Using a polar coordinate system, the problem of finding the aortic boundary reduces to a horizontal boundary detection which can be efficiently computed using the dynamic programming method. The polar image is computed by considering the centroid of the detected aortic circle as the origin and the radial extent twice the radius of the detected aortic circle. A non-linear gray-scale modification is performed followed by anisotropic diffusion to enhance blood and suppress the rest of the tissues. The aortic boundary is detected by computing an optimal horizontal path between the two ends of the polar image. We use a similar dynamic programming approach as in Section 2.1.2, with the difference being the formulation of the problem. In this case, the optimal path is represented as a polyline with L vertices $(Q_1, Q_2, Q_3, \dots, Q_L) \in Q$. Also, the cost function for the polar image is expressed as:

$$C(Q_i) = -\omega_d C_d(Q_i) - \omega_g C_g(Q_i) - \omega_r C_r(Q_{i-1}, Q_i),$$

where ω_d , ω_g , and ω_r are the weights for the intensity cost component term C_d , the vertical gradient cost component term C_g , and the continuity cost component term C_r corresponding to vertical distance between pixels on the polyline in adjacent columns of the polar image, respectively. The intensity cost component term forces the boundary to follow the homogeneous path through the pixels with higher blood intensity values. The gradient cost component term is responsible for moving the boundary towards the points having strong gradient value in a direction perpendicular to the boundary. The continuity cost component term restricts the boundary from taking big steps in the radial direction between the adjacent pixels along the horizontal boundary. This term imposes the spatial continuity constraint, smoothing out

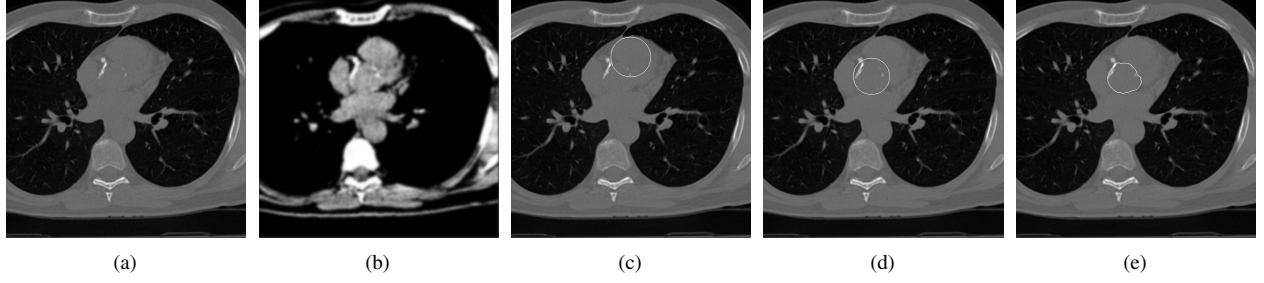


Fig. 1. (a) Unprocessed original CT image, (b) pre-processed enhanced image, (c) detected circle as global maximum in Hough space, (d) detected circle using dynamic programming, and (e) boundary contour detected by dynamic programming.

the boundary in the horizontal direction. The continuity term can be implemented either as the linear or the second order continuity term. The second order term allows smoother transitions of the boundary in the vertical direction. The detected boundary is transformed back into Euclidean coordinates, providing the refined aortic boundaries (Fig. 1(e)).

3. RESULTS AND DISCUSSION

Dataset: The proposed method was applied on 37 randomly selected cardiac non-contrast CT scans. The images were acquired on an electron-beam CT (EBCT) scanner (GE Imatron). For each scan, a stack of 20-36 contiguous slices, with slice thickness of 3mm each, covering the heart were acquired. Each image was reconstructed to 512×512 pixels with a gray value resolution of 16-bit. The pixel sizes ranged from 0.508mm to 0.586mm.

3.1. Validation results

The proposed localization and segmentation methods are evaluated by comparing the obtained results with aorta boundaries manually annotated by an expert.

3.1.1. Localization of Aorta

To assess the accuracy of the dynamic programming-based aorta localization method (HD), the centroid (c_m) and average radius (r_m) of manually annotated boundary contours are determined first. The centroid c_m of the manual contour (B_m) is treated as the gold standard for aorta position for validation purposes. Next, we compute the distance (δ_α) between the centroid (c_m) and the center point estimate (c_α) obtained in Section 2.1.2. A figure of merit, the relative square distance error (D_α), is defined as the ratio of the squared distance between the two aortic positions and the squared average radius, $D_\alpha = \delta_\alpha^2 / r_m^2$. The measure D_α is used to determine if the automatically detected aortic center point c_α falls inside the manual aortic contour B_m or not. If $D_\alpha < 1$, then c_α is inside B_m indicating success, else c_α is outside indicating a failure. The D_α also gives a measure of accuracy of localization by determining how close the automatically estimated position is to the manually estimated position relative to the size of the manual contour. The lower the value of D_α , the greater is

the accuracy of the method in determining the aortic position. Figure 2 depicts the cumulative D_α (solid line) for the proposed dynamic programming-based aorta localization method (HD) and compares it against the cumulative D_g (dashed line) of commonly used method of selecting the global maxima point in Hough space (HG). The locations of ascending and descending aortas were estimated inside the manually annotated contours in 94% and 100% of cases, respectively, by the HD method as compared to 71% and 85% of cases, respectively, by the HG method. In 6% of the cases, our method could not locate the ascending aorta because the pulmonary artery exhibited stronger edge responses. However, this can be easily corrected by either incorporating a priori knowledge of aorta location relative to the lungs or by placing a starting point manually inside the aorta to guide the dynamic programming algorithm.

3.1.2. Segmentation of Aorta

Our automated aorta segmentation method was assessed for boundary error and volume overlap. The convexity of the aorta allows us to use the root mean squared radial distance (R) between the boundaries as a boundary error metric. The boundary contours are parameterized over θ with the centroid c_m of the manual contour being the center of rotation. The error metric R is computed as a root mean square distance between corresponding points on the manual and automated boundary contours obtained from the intersections of the radial lines drawn outward from the centroid to the boundary contours. The radial distance error R effectively captures the error on the aortic segmentation. Figure 3 depicts the cumulative radial distance errors between automatic and manual contours for ascending and descending aorta for the proposed segmentation method (Fig. 3, solid line). To illustrate the requirement of this additional dynamic programming-based boundary refinement step (Sec. 2.2), we compare the segmentation results against the Hough circles extracted in the localization step (Sec. 2.1.2) (Fig. 3, dashed line). It can be observed that the refined contours follow the aortic boundary more closely than the Hough circles in 86% and 100% of the cases for the ascending and descending aorta. The 14% of the cases in which the automated method exhibits infe-

Table 1. Descriptive statistics of the Dice similarity coefficient for aorta volume overlap.

	DSC	DSC Range
Ascending	0.88 ± 0.08	[0.68, 0.96]
Descending	0.96 ± 0.01	[0.91, 0.97]

rior results for ascending aorta segmentation are mostly near the aortic root where the aortic shape, size and tissue contrast with surroundings changes significantly. These results can be improved by incorporating 3D surface continuity factor in the dynamic programming algorithm such that the slices suffering from low contrast can benefit from stronger edge responses from the neighboring slices.

The volume overlap is estimated in terms of a well-known overlap measure, Dice similarity coefficient (DSC), $DSC(S_m, S_a) = \frac{2|S_m \cap S_a|}{|S_m| + |S_a|}$, where S_m and S_a represent manual and automated segmentation methods, and $|X|$ denotes the number of voxels labeled by X . Table 1 provides descriptive statistics of the DSC measure obtained for the ascending and descending aorta by the automated method.

4. CONCLUSION

A dynamic programming-based method for the automated localization and segmentation of the thoracic aorta is presented in this paper. Using the Hough space as a medialness feature space and applying dynamic programming for tracking, provides an automatic and robust method to detect the center-line of symmetric and tubular structures like the aorta. It is shown that this step introduces a significant improvement in the localization of the aorta compared to the general approach of selecting the point of global maxima in the Hough space. The dynamic programming-based aorta segmentation results compare well with manually traced aorta boundaries. However, segmentation of ascending aorta can be further improved by incorporating 3D surface continuity constraints and allowing more flexibility to deviate from circular shape assumption. We are now investigating methods to improve the ascending aorta segmentation specifically.

Acknowledgment

This work was supported in part by NSF Grant IIS-0431144. Any opinions, findings, conclusions or recommendations expressed in this material are those of the authors and may not reflect the views of the NSF. Ms. O.C. Avila-Montes is an intern from the Biomedical Engineering Program, Antioquia School of Engineering, Envigado, Antioquia, Colombia.

5. REFERENCES

[1] N. Rodondi, B.C. Taylor, D.C. Bauer, L.Y. Lui, M.T. Vogt, H.A. Fink, W.S. Browner, S.R. Cummings, and

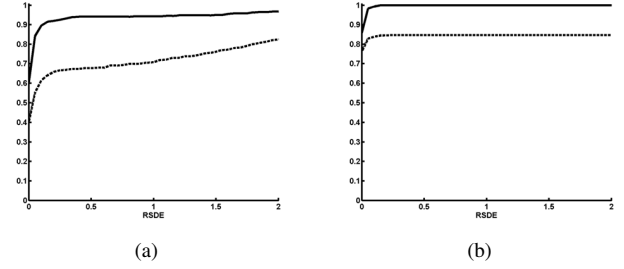


Fig. 2. Cumulative localization error, D obtained by the dynamic programming-based selection method (solid line) and the global maximum selection method (dashed line) for (a) the ascending aorta and (b) the descending aorta.

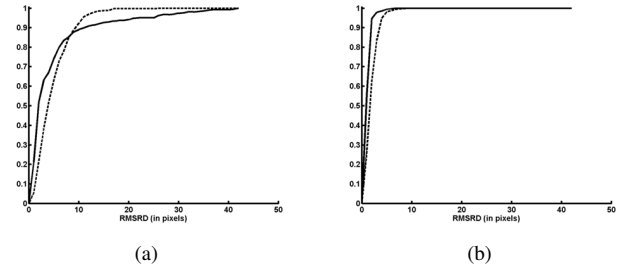


Fig. 3. Cumulative radial distance error, R , of the dynamic programming-based segmentation method (solid line) and the Hough circle selected in localization step (dashed line) for (a) the ascending aorta and (b) the descending aorta.

K.E. Ensrud, "Association between aortic calcification and total and cardiovascular mortality in older women," *J Intern Med*, vol. 261, no. 3, pp. 238–244, 2007.

[2] J.C. Witteman, F.J. Kok, J.L. van Saase, and H.A. Valkenburg, "Aortic calcification as a predictor of cardiovascular mortality," *Lancet*, vol. 2, no. 8516, pp. 1120–1122, 1986.

[3] P. Raggi, T.Q. Callister, B. Cooil, Z.X. He, N.J. Lippolis, D.J. Russo, A. Zelinger, and J.J. Mahmarian, "Identification of patients at increased risk of first unheralded acute myocardial infarction by electron-beam computed tomography," *Circulation*, vol. 101, no. 8, pp. 850–855, 2000.

[4] D. Rueckert, P. Burger, S.M. Forbat, R.D. Mohiaddin, and G.Z. Yang, "Automatic tracking of the aorta in cardiovascular MR images using deformable models," *IEEE Trans Med Imaging*, vol. 16, no. 5, pp. 581–590, 1997.

[5] I.M. Adame, R.J. van der Geest, D.A. Bluemke, J.A. Lima, J.H. Reiber, and B.P. Lelieveldt, "Automatic vessel wall contour detection and quantification of wall thickness in in-vivo MR images of the human aorta," *J Magn Reson Imaging*, vol. 24, no. 3, pp. 595–602, 2006.

[6] P. Perona and J. Malik, "Scale-space and edge detection using anisotropic diffusion," *IEEE Trans. Pattern Anal. Mach. Intell.*, vol. 12, no. 7, pp. 629–639, 1990.